Two-dimensional particle-in-cell plasma source ion implantation of a prolate spheroid target*

Liu Cheng-Sen(刘成森)[a)†], Han Hong-Ying(韩宏颖)[a)], Peng Xiao-Qing(彭晓晴)[a)], Chang Ye(昶 叶)[a)], and Wang De-Zhen(王德真)[b)]

[a)] *College of Physics and Electronic Technology, Liaoning Normal University, Dalian* 116029, *China*
[b)] *State Key Laboratory for Materials Modification by Laser, Ion and Electron Beams, School of Physics and Optoelectronic Technology, Dalian University of Technology, Dalian* 116023, *China*

(Received 3 July 2009; revised manuscript received 13 August 2009)

A two-dimensional particle-in-cell simulation is used to study the time-dependent evolution of the sheath surrounding a prolate spheroid target during a high voltage pulse in plasma source ion implantation. Our study shows that the potential contour lines pack more closely in the plasma sheath near the vertex of the major axis, i.e. where a thinner sheath is formed, and a non-uniform total ion dose distribution is incident along the surface of the prolate spheroid target due to the focusing of ions by the potential structure. Ion focusing takes place not only at the vertex of the major axis, where dense potential contour lines exist, but also at the vertex of the minor axis, where sparse contour lines exist. This results in two peaks of the received ion dose, locating at the vertices of the major and minor axes of the prolate spheroid target, and an ion dose valley, staying always between the vertices, rather than at the vertex of the minor axis.

Keywords: plasma source ion implantation, ion sheath, two-dimensional particle-in-cell model, Ion dose

PACC: 5240K, 5265, 5275R

1. Introduction

Plasma source ion implantation (PSII) is an efficient surface treatment and material synthesis technique, and it has been successfully used to increase the hardness and wear resistance of industrial components, improve the biocompatibility of medical implants, and synthesize biocompatible titanium oxide on artificial heart values and blood vessels.[1−11] Because there is no line-of-sight restriction, it is also an excellent technique to treat large and irregular components, such as aerospace bearings,[12] inner surface of bores,[13−16] gears,[17] and hemispherical bowl-shaped containers.[18,19] In the PSII process, ions are accelerated by a negative voltage applied to the target, and implanted through the plasma sheath. In practice, PSII into targets with complex geometries must be conducted carefully, because the ion sheath may not be conformal if the conditions are improper. Experimental and numerical investigations have been conducted to investigate the effects of the processing parameters and target shape on the sheath propagation dynamics and resulting ion-dose distributions.

A prolate spheroid is used in the design of many artificial flying targets because of the shape's excellent aerodynamics.[20,21] To further improve the surface properties, e.g. enhancing temperature capabilities or reducing air resistance, the PSII is often used, due to such advantages as high efficiency and small instrument footprint. In this paper, we use the two-dimensional particle-in-cell (PIC) model to investigate the PSII process of a prolate spheroid target. Our results show that the ion dose along the implanted surface is non-uniform. An ion dose peak is observed at the vertex corresponding to the long axis of the prolate spheroid, and a minimum dose emerges at some points between the two vertices of the semimajor and semiminor axes of the prolate spheroid.

2. Model

We consider the PSII into the surface of a prolate spheroid as shown in Fig. 1. a is the semimajor axis and b is the semiminor axis of the prolate spheroid ($b < a$). The system is rotationally invariant about

*Project supported by the Program for Innovative Research Team of High Education in Liaoning Province, China (Grant No. 2009T055).
†Corresponding author. E-mail: lchs@vip.sina.com
© 2010 Chinese Physical Society and IOP Publishing Ltd

the semimajor axis of the spheroid, and it is symmetric with respect to the plane including the semiminor axis, so the simulated region is a quarter of the rectangular transverse section that includes the semimajor axis of the spheroid as shown in Fig. 1.

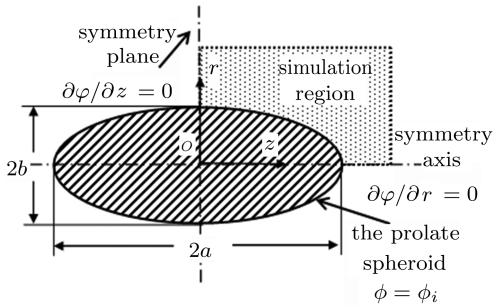


Fig. 1. Schematic diagram of the implantation geometry considered.

The prolate spheroidal workpiece is immersed in a charge-neutral plasma, in which the ion and electron densities n_i and n_e are both equal to the plasma density n_0, i.e. $n_\mathrm{i} = n_\mathrm{e} = n_0$. The potential is initially $\phi = 0$ everywhere in the simulation region. The target potential is given by

$$\phi(t) = \begin{cases} \phi_p(t/t_r), & t \le t_r, \\ \phi_p, & t > t_r \end{cases} \tag{1}$$

to induce the formation of an ion-matrix sheath. Electrons are repelled from the target. Ions are initially at rest, since the ion mass is much larger than the electron mass. When $t > \omega_{\mathrm{pe}}^{-1}$ (inverse electron plasma frequency), ions are accelerated by the electric field in the sheath, and implanted into the target until the applied voltage pulse is over. In the simulation, the ions are assumed to be noncollisional, cold (low pressure PSII conditions), and accelerated only by the electric field. The electrons are in thermal equilibrium and the electron density n_e is given by the Boltzmann relationship

$$n_\mathrm{e} = n_0 \exp\left(\frac{e\phi}{kT_\mathrm{e}}\right), \tag{2}$$

where n_0 is the initial ion density, k is Boltzmann's constant, and T_e is the electron temperature. Thus, we only need to follow the ion dynamics. Poisson's equation relates the potential ϕ to the electron density n_e and ion density n_i through the equation

$$\nabla^2\phi = -\frac{e}{\varepsilon_0}(n_\mathrm{i} - n_\mathrm{e}), \tag{3}$$

where ε_0 is the permittivity in free space and e is the electron charge. The ions are accelerated by the electric field and their motion is described by Newton's equations of motion. The ion trajectories are determined by the following equations:

$$v_r(f) = v_r(I) - \frac{q}{M}\frac{\partial\phi}{\partial r}\Delta t, \tag{4}$$

$$v_z(f) = v_z(I) - \frac{q}{M}\frac{\partial\phi}{\partial z}\Delta t, \tag{5}$$

$$\Delta r = v_r(I)\cdot\Delta t - \frac{1}{2}\frac{q}{M}\frac{\partial\phi}{\partial r}(\Delta t)^2, \tag{6}$$

$$\Delta z = v_z(I)\cdot\Delta t - \frac{1}{2}\frac{q}{M}\frac{\partial\phi}{\partial z}(\Delta t)^2, \tag{7}$$

where q is the ion charge, M is the ion mass. $v_z(f)$ and $v_z(I)$ are the velocities along the z direction, and $v_r(f)$ and $v_r(I)$ are the velocities along the r direction, before and after the time step Δt, respectively. The plasma quantities can be made dimensionless in cylindrical coordinates by normalization, and Eqs. (3)–(7) can be solved by finite difference.[22] In the simulation, it is assumed that the top and right boundaries of the simulation region are connected by a neutral plasma, so $\varphi = 0$. At the left boundary $\partial\varphi/\partial z = 0$, and at the bottom boundary $\partial\varphi/\partial r = 0$. Initially, the plasma density in the simulation region, n, is 1, i.e. $n = 1$.

3. Results and discussion

The lengths of the semimajor axis and semiminor axis of the prolate spheroid are $a = 29.7$ cm and $b = 9.9$ cm respectively. For the illustrative purpose, we choose plasma density $n_0 = 6.8\times10^9$ cm^{-3}, singly ionized argon ions Ar^+, and $T_\mathrm{e} =$ 1.5 eV. The applied potential to the target is initially zero and rises (becoming increasingly negtive) at a rate of 120 kV/μs, until it reaches a plateau value of -60 kV and maintains this value. The other simulation parameters are as follows: a square grid spacing of 3.3 mm and a time step of 2.5×10^{-4} μs. The area of one cell is 10.89 mm^2. The maximum simulation area is 59.4×89.1 cm^2, and a total of 72000 cells are considered. One hundred particles (ions) are initially uniformly placed in each cell. The simulation duration is 4.5 μs.

The temporal evolution of the normalized potential contour lines is displayed in Fig. 2 at 0.5 (a), 2.0 (b), 4.0 (c), and 4.5 μs (d). The plasma sheath forms quickly around the prolate spheroid from the beginning of the applied voltage pulse. The potential contour lines pack more closely in the sheath near the

vertex of the semimajor axis, i.e. where a thinner sheath is formed.

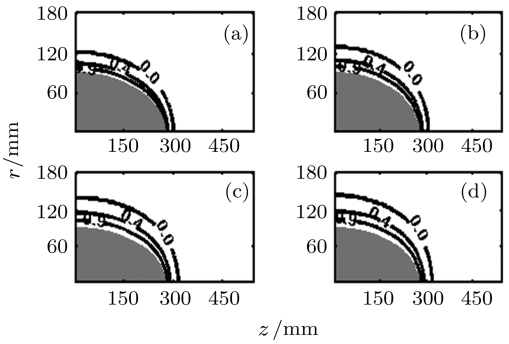


Fig. 2. Temporal evolution of the normalized potential contours.

Figure 3 shows the temporal evolutions of the ion density contours. The focusing effect of the plasma sheath can be observed, which causes ions to converge near the vertex of the semimajor axis; the expansion of the plasma sheath is smallest here. This is consistent with the fact that higher ion density leads to a thinner sheath and a smaller expansion velocity.

In Fig. 4(a), we show the velocity vectors as arrows in four samples each with 100 ions for $t = 4.5$ μs, Figure 4(b) is a local enlargement of Fig. 4(a), so as to clearly show the ion movement. Longer arrows near the target surface represent larger ion velocity. It is apparent that an ion is accelerated by the electric field while traveling from the sheath edge to the target, and therefore, its velocity is gradually increased. It can also be observed that the focusing effect causes the ion direction of motion not to be perpendicular to the target surface; or rather, it seems to force the ions to converge toward the vertex of the semimajor axis of the spheroid as shown in Fig. 5.

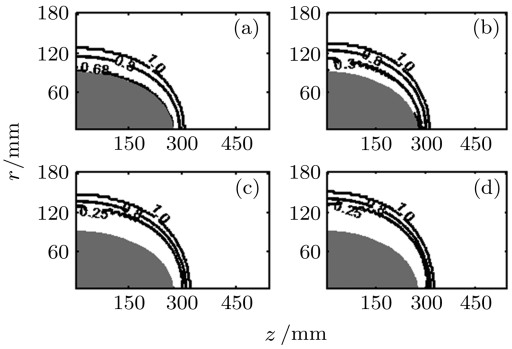


Fig. 3. Temporal evolutions of the normalized ion density contours.

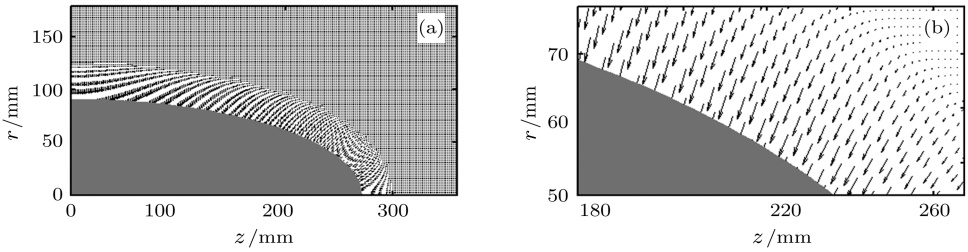


Fig. 4. Ion velocity vector distribution denoted as arrows (a) and its local enlargement (b).

The time evolutions of the total incident ion dose along the surface of the prolate spheroid at different times are displayed in Fig. 5. The surface of the prolate spheroid is not evenly implanted in the whole PSII process, because of ion focusing effects by the electric field near the vertices. More ions are implanted into the vertex regions corresponding to the axes, and thereby the largest dose is received on the vertex. The ion dose decreases gradually along the surface of the spheroid, and an ion dose valley is found to be about 85% of the whole surface length away from the vertex of the semimajor axis, and maintains this position throughout the duration of the pulse. It is obvious that the total incident ion dose along the surface increases with time goes on, and the distribution relation almost remains constant.

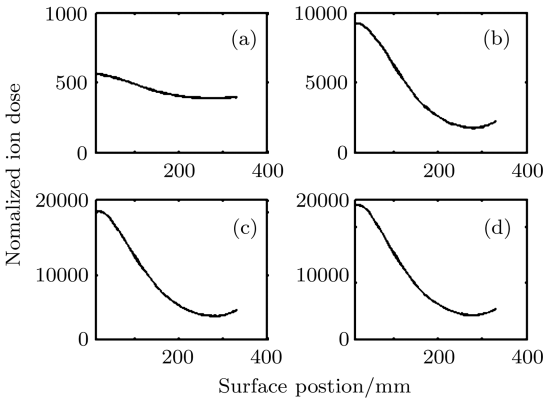


Fig. 5. Total incident ion dose along the spheroid surface from the vertex of the semimajor axis to the semiminor axis at 0.5 (a), 2.0 (b), 4.0 (c), and 4.5 μs (d).

4. Conclusion

We present a two-dimensional PIC model to study the PSII of a prolate spheroid target. Our results demonstrate an ion focusing effect, which leads to nonuniformity of the incident ion dose on the surface of the implanted prolate spheroid. Ion focusing occurs not only at the vertex of the major axis, but also at the vertex of the minor axis. The higher one between the two ion dose peaks is located at the vertex of the major axis, and the other is at the vertex of the minor axis. An ion dose valley always stays between the vertices, and closer to the vertex of the minor axis. The results demonstrate that ion focusing originates from the plasma sheath structure, which is time- and space-independent for a prolate spheroid target in the case we studied.

References

[1] Conrad J R, Radtke J L, Dodd R A, Worzala F J and Tran N C 1987 *J. Appl. Phys.* **62** 4591

[2] Scheridan T E and Alport M J 1994 *Appl. Phys. Lett.* **64** 1783

[3] Mantese J V, Brown I G, Cheung N W and Collins G A 1996 *MRS Bull.* **21** 52

[4] Chu P K, Qin S, Chan C, Cheung N W and Larson L A 1996 *Mater. Sci. Eng.* R **17** 207

[5] Kwok D T K, Chu P K and Chan C 1998 *IEEE Trans. Plasma Sci.* **26** 1669

[6] Tian X B, Fu R K Y, Chu P K and Yang S Q 2005 *Surf. Coatings Technol.* **196** 162

[7] Shao J, Jones E C and Cheung N W 1997 *Surf. Coat. Technol.* **93** 254

[8] Ayers R A, Simske S J, Bateman T A, Petkus A, Sachdeva R L C and Gyunter V E 1999 *J. Biomed. Mater. Res.* **45** 42

[9] Ikeda D, Ogawa M, Hara Y, Nishimura Y, Odusanya O, Azuma K, Matsuda S, Yatsuzuka M and Murakami A 2002 *Surf. Coat. Technol.* **156** 301

[10] Chu P K, Chen J Y, Wang L P and Huang N 2002 *Mater. Sci. Eng.: Rep.* **36** 143

[11] Liu X, Chu P K and Ding C 2004 *Mater. Sci. Eng.: Rep.* **47** 49

[12] Wang S Y, Chu P K, Tang B Y, Zeng X C and Wang X F 1997 *Nucl. Instrum. Methods Phys. Res.* B **127** 100

[13] Sheridan T E 1993 *J. Appl. Phys.* **74** 4903

[14] Zeng X C, Tang B Y and Chu P K 1996 *Appl. Phys. Lett.* **69** 3815

[15] Zeng X C, Kwok T K, Liu A G, Chu P K and Tang B Y 1998 *J. Appl. Phys.* **83** 44

[16] Liu C S and Wang D Z 2003 *Acta Phys. Sin.* **52** 109 (in Chinese)

[17] Zeng Z M, Kwok T K, Tian X B, Tang B Y and Chu P K 1999 *J. Appl. Phys.* **86** 120

[18] Liu C S and Wang D Z 2003 *Surf. Coat. Technol.* **171** 119

[19] Liu C S, Wang Y H and Wang D Z 2005 *Chin. Phys.* **14** 163

[20] Knapp D G 2002 *Proc. SPIE* **4832** 394

[21] Sun J X, Sun Q, Li D X and Lu Z W 2003 *Acta Phys. Sin.* **56** 3900 (in Chinese)

[22] Liu C S, Wang D Z, Liu T W and Wang Y H 2008 *Acta Phys. Sin.* **57** 6450 (in Chinese)